

Nondivergent calculation of unwanted high-order tunneling rates in single-electron devices

P. Lafarge and D. Esteve

*Service de Physique de l'Etat Condensé, Commissariat à l'Energie Atomique Saclay,
F-91191, Gif-sur-Yvette Cedex, France*

(Received 26 May 1993)

Recently developed single-electron devices are based on the control of electron tunneling across each tunnel junction of the circuit. However, unwanted higher-order tunneling processes, referred to as cotunneling processes, modify this simple picture and reduce the accuracy of the devices. We calculate the cotunneling rate in a linear array of tunnel junctions beyond the lowest order of perturbation theory by partially resumming the infinite perturbation expansion for the energy of a metastable state. We apply this calculation to the transition between two different tunneling regimes in various single-electron circuits.

I. INTRODUCTION

In recent years the Coulomb blockade of tunneling has opened a new field of electronics referred to as "single electronics."¹ The first realizations are ultrasensitive electrometers² or charge-transferring devices such as turnstiles and pumps,^{3,4} the latter being a potential candidate for a dc current standard. A single-electron device consists of small metallic islands separated by ultrasmall tunnel junctions with tunnel resistance R_t larger than the resistance quantum $R_K = h/e^2$. Control voltage sources are also applied to the islands through gate capacitors. Each island has a total capacitance C_{island} such that the electrostatic energy of a single excess electron $e^2/2C_{\text{island}}$ is larger than the characteristic energy $k_B T$ of the thermal fluctuations. Under these conditions, the number of electrons inside each island is a good quantum number with negligible thermal fluctuations.⁵ Single-electron tunneling through each junction can be forced or blocked by setting the control voltages to suitable values. However, higher-order tunneling processes can directly transfer a single charge across two or more tunnel junctions and therefore compromise the proper operation of the device. This phenomenon, discovered by Averin and Odintsov⁶ and called here cotunneling, allows one electron charge to be transferred through k tunnel junctions, although single-electron tunneling across each junction is forbidden. The simplest circuit which exhibits cotunneling is the single-electron transistor which consists of two tunnel junctions in series. Cotunneling is responsible for the leakage current which is observed when this circuit is biased inside the Coulomb gap.^{7,8} For the sake of completeness, let us mention that a single junction biased by a current source should also exhibit a Coulomb gap.¹ In this case, subgap leakage can arise from imperfect current biasing⁹ or from the transient electronic rearrangement during the tunneling process.¹⁰

In a linear array of N tunnel junctions biased with a voltage source V , a cotunneling event that transfers one electron across the whole array in the direction of increasing potential is always possible (see Fig. 1). In this

paper we will consider the case where another tunneling transition of lower order becomes energetically allowed. A second tunneling process at the P th order, with $P < N$, takes place in the array. Both transitions start from the same initial state and transfer one electron in the same direction, but the final states are different. Because it is a perturbative approach, the original cotunneling theory can only give an expression for the rate of the lowest-order decay process which is energetically allowed in the array. In order to describe the behavior of the array when another tunneling transition can occur, we have derived a nondivergent expression of the quantum decay

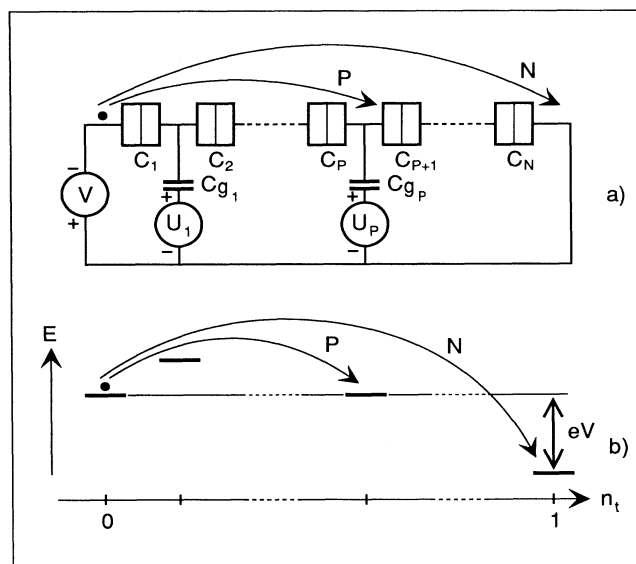


FIG. 1. (a) Schematic of a linear array of N tunnel junctions. The rectangular symbols represent ultrasmall tunnel junctions. (b) Energy states of the circuit when the electrostatic energy of the P th intermediate state of an N th-order cotunneling transition is equal to the initial-stage energy. n_i is the number of electrons which have passed through the array. The arrows indicate cotunneling events through N or P junctions.

rate of the initial state by partially resumming the perturbation expansion. We will consider here three physical devices where the crossover between two tunneling transitions with different orders currently appears: (i) the single-electron transistor consisting of two tunnel junctions in series, the simplest example of a linear array ($P=1, N=2$). Our calculations are in good agreement with results obtained by other approaches;¹¹⁻¹³ (ii) the more general case of a linear array of N tunnel junctions, for which we aim at describing the effect of a finite transport voltage ($P=N-1, N>2$); and (iii) the charge-transferring devices such as turnstiles and pumps. In that kind of circuit, every step of a transfer cycle is exposed to an unwanted cotunneling event through the array ($P=1, N>2$) and the accuracy of the transfer is affected by the rate of this leakage process.

II. THE PERTURBATIVE THEORY OF COTUNNELING

Before examining the case of the single-electron transistor, it is worthwhile to describe the general perturbative theory of cotunneling. Following Averin and Odintsov,⁶ a cotunneling transition that transfers one electron through a linear array of N tunnel junctions can be described by an arbitrary sequence of N single tunneling events $\{j_1, \dots, j_k, \dots, j_N\}$ where j_k denotes the position in the array of the k th tunneling event. When a tunneling event occurs on the j_k th junction, one electron leaves a filled state at ϵ_l below the Fermi level on one side of the junction and occupies an empty state at ϵ_r above the Fermi level on the other side. It creates an "electron-hole" excitation of energy $\epsilon = \epsilon_r + \epsilon_l$. Note,

however, that here the electron and the hole are not in the same piece of metal. In the following, such an excitation will be referred to as a "tunneling exciton" of energy ϵ ; the tunneling exciton density of states is $\rho(\epsilon) = \lambda\epsilon$. Within the tunnel Hamiltonian approach, λ and the tunnel matrix element t are related to the junction tunnel resistance R_t by

$$\lambda t^2 = R_K / 4\pi^2 R_t. \quad (1)$$

Since the final expression of the cotunneling rates depends on the parameters λ and t of each junction only through the combination λt^2 , we use, for the sake of clarity, the same λ for all junctions. The conservation of energy implies that the sum of the energies of all the tunneling excitons involved in a cotunneling process must be equal to the electrostatic energy difference ΔE between the initial and the final state of the transition. Therefore, at $T=0$, only transitions bringing the system in a state of lower energy than the initial one are allowed. Let us assume that the energetically allowed transition with lowest order is a cotunneling transition across M junctions. For a given sequence $\{j_1, \dots, j_M\}$ of M single tunneling events there are $M-1$ intermediate virtual states $\{s_1, \dots, s_{M-1}\}$. After K steps in the sequence $\{j_1, \dots, j_M\}$ the system is in the state s_k and its energy is given by the sum of the electrostatic energy $E(s_k)$ relative to the energy of the initial state and the energies of the tunneling excitons created by previous tunneling events on junctions j_1, \dots, j_k . The M cotunneling rate Γ_M calculated by the perturbative theory of cotunneling⁵ is given by

$$\Gamma_M = \frac{2\pi}{\hbar} \left(\prod_{i=1}^M \frac{R_K}{4\pi^2 R_{t_i}} \right) \int_0^{+\infty} S^2(\epsilon_1, \dots, \epsilon_M) \delta \left(\Delta E - \sum_{i=1}^M \epsilon_i \right) \prod_{i=1}^M \epsilon_i d\epsilon_i$$

$$\text{where } S(\epsilon_1, \dots, \epsilon_M) = \sum_{\{j_1, \dots, j_M\}} \prod_{k=1}^{M-1} \left[E(s_k) + \sum_{i=1}^k \epsilon_i \right]^{-1}. \quad (2)$$

This integral cannot be analytically calculated except for two junctions in series. In the limit where ΔE is much smaller than the intermediate state energies $E(s_k)$, a useful approximation is obtained by setting the tunneling exciton energies in the energy denominators to zero. In this approximation the M cotunneling rate takes the form

$$\Gamma'_M = \frac{2\pi}{\hbar} \left(\prod_{i=1}^M \frac{R_K}{4\pi^2 R_{t_i}} \right) S'^2 \frac{\Delta E^{2M-1}}{(2M-1)!}$$

$$\text{where } S' = \sum_{\{j_1, \dots, j_M\}} \prod_{k=1}^{M-1} [E(s_k)]^{-1}. \quad (3)$$

We now consider a linear array of N tunnel junctions biased with a voltage source V . Gate voltages V_{g_i} are also applied to the $N-1$ islands of the array through gate capacitors C_{g_i} . In such a circuit an N th-order cotunneling transition, hereafter called an N tunneling transition, is always possible. Even in the Coulomb blockade regime

the transition can occur because the change of electrostatic energy due to the transfer of one electron across the whole array is $-eV$. If under the effect of the gate voltages one of the intermediate state energy $E(s_p)$ with $P < N$ vanishes, then a P tunneling transition becomes possible (see Fig. 1). The perturbative expression (2) can only be used to evaluate the rate of the lowest-order transition, i.e., an N tunneling rate if $E(s_p) > 0$ or a P tunneling rate if $E(s_p) < 0$. But the crossover between N and P tunneling is not properly described. Moreover, in the particular case $P=1$, the N tunneling rate diverges at the threshold while the single tunneling rate is zero at the threshold.

III. PARTIAL RESUMMATION OF THE PERTURBATION EXPANSION IN THE CASE OF THE SINGLE-ELECTRON TRANSISTOR

The simplest example of linear arrays that exhibits the crossover between two tunneling transitions at different

orders is the single-electron transistor (Fig. 2). This device consists of two tunnel junctions in series of capacitances C_1 and C_2 and tunnel resistances R_{t_1} and R_{t_2} connected to a transport voltage source V . A gate voltage U is also capacitively coupled to the central electrode by a capacitor C_g . The state of the device is completely described by the number n of excess electrons on the central island and the number n_t of electrons having passed through the voltage source V . For a given state the energy of the whole system including the voltage sources is $E(n, n_t) = (ne - C_g U)^2 / 2C_\Sigma - (C_g U)^2 / 2C_\Sigma - n_t eV$, where $C_\Sigma = C_1 + C_2 + C_g$. For $0 < V < e/C_\Sigma$ and $0 < C_g U < e/4$, we can limit the state space to four states which we denote (0), (1), (-1), and (0)*. The initial state (0) corresponds to $n = n_t = 0$. The states (1) and (-1) differ from the initial state (0) by a tunneling event on the first and the second junction, respectively. The state (0)* differs from (0) by one electron having passed through the device. The energy of (0)* is $-eV$ and the energies of (1) and (-1) are equal to $E_1 = E(1, 0)$ and $E_2 = E(-1, 0)$, respectively. For $V < V_{th}$, where V_{th} is a threshold voltage dependent on the voltage U and the capacitances C_1 , C_2 , and C_g , E_1 and E_2 are positive and the tunneling of one electron across each junction is suppressed. Nevertheless, there is a finite current through the device due to the decay of (0) to (0)*. The cotunneling transition (0) \rightarrow (0)* can take place through two channels: (0) \rightarrow (1) \rightarrow (0)* or (0) \rightarrow (-1) \rightarrow (0)* (Fig. 3). At $V = V_{th}$, one of the intermediate energies E_1 or E_2 vanishes. The cotunneling rate calculated using Eq. (2) presents at the threshold a logarithmic divergence which can be regularized.^{11,12} Above the threshold, electrons can be transferred by a sequence of allowed single tunneling transitions. The limiting single transition rate is proportional to E_1 or E_2 and therefore starts from zero. In order to properly obtain the crossover between the cotunneling and single tunneling regimes, we calculate directly the decay rate of the initial state (0) without specifying the final state. This decay rate is a good approximation of the tunneling rate across the whole array if the occupancy probability of the intermediate states (1) and (-1) is much smaller than 1. This condition corresponds to $0 < V \leq 1.5V_{th}$. At higher voltage, one can use the simplified master equation approach,¹⁴ which only considers single tunneling events on each junction and which

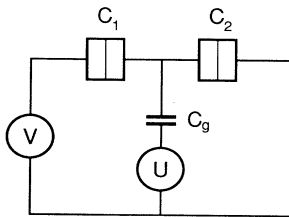


FIG. 2. Circuit diagram of the single-electron transistor which consists of two small tunnel junctions of capacitances C_1 and C_2 biased with a voltage source V . A control voltage source U is capacitively coupled to the island formed between the junctions.

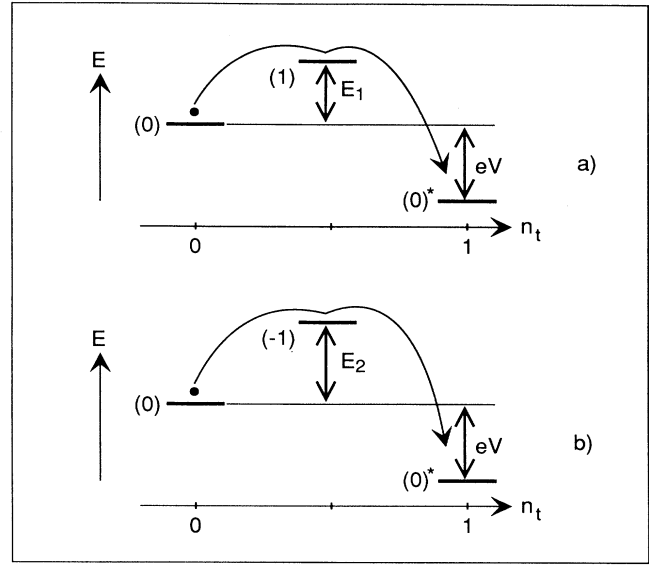


FIG. 3. Energy states of the single-electron transistor when the circuit is in the Coulomb blockade regime. The arrows indicate cotunneling transitions. A cotunneling transition between the initial (0) and the final state (0)* can take place through two channels (a) and (b).

becomes sufficiently accurate.

To express the quantum decay rate of the (0) state we use the formalism of the energy displacement operator $R(z)$.¹⁵ The decay rate of the initial state $|i\rangle$ is related to $R(z)$ by

$$\Gamma = -\frac{2}{\hbar} \text{Im}[PR(E_i + i\eta)P], \quad (4)$$

where $P = |i\rangle\langle i|$, E_i is the energy of the initial state, and $\eta \rightarrow 0^+$. The perturbative expansion of $R(z)$ is

$$R(z) = H_T + H_T \frac{Q}{z - H_0} H_T + H_T \frac{Q}{z - H_0} H_T \frac{Q}{z - H_0} H_T + \dots, \quad (5)$$

where $Q = 1 - P$, H_T is the tunnel Hamiltonian and H_0 is the sum of the electrostatic Hamiltonian of the whole circuit and of the tunneling exciton kinetic-energy Hamiltonian. Each term in the PRP series corresponds to a path in the state space and can be represented by a diagram (see Fig. 4). The construction rules of such a diagram are as follows: an upward curved line represents a tunneling exciton excitation on the first junction and a downward curved line a tunneling exciton on the second junction. Each vertex corresponds to a transition between two different states of the system by absorption or emission of a tunneling exciton. In the calculation associated with the diagram, each section, i.e., portion of a diagram contained between two dotted lines, contributes by an energy denominator and each vertex by a tunnel ma-

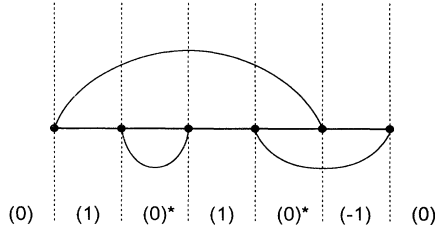


FIG. 4. General form of a diagram. An upward (downward) arc represents a tunneling exciton excitation on the first (second) junction of the single-electron transistor. The solid dots correspond to the absorption or the emission of a tunneling exciton. Each section of the diagram contained between two dashed lines corresponds to a given state of the device.

trix element. Finally there is an integration over all the tunneling exciton energies $\varepsilon_1, \dots, \varepsilon_i$ of the diagram with densities of states $\lambda\varepsilon_1, \dots, \lambda\varepsilon_i$. Only paths starting from the (0) state and coming back to (0) solely at the end give nonvanishing terms in the series (5). Each diagram containing one tunneling exciton [Fig. 5(a)] gives, at $V > V_{th}$, the single tunneling rate through the corresponding junction of the single-electron transistor. The set of diagrams containing two tunneling excitons depicted in Fig. 5(b) give, at $V < V_{th}$, the perturbative expression of the cotunneling rate. A horizontal segment, which is located under or over one tunneling exciton arc, corresponds, respectively, to the (1) state or the (-1) state (see Fig. 4). In the upper left diagram of Fig. 5(b), a segment (1) appears twice under the tunneling exciton denoted ε_1 . The same situation is reproduced in the upper right diagram of Fig. 5(b) with a segment (-1) over the tunneling exciton ε_2 . In these two diagrams, the horizontal segments corresponding to the (-1) or (1) state are the origin of the cotunneling rate divergence because the corresponding sections contribute by the square of energy denominators which vanish at the threshold. More generally, for a given number of tunneling excitons the divergence order of a diagram is proportional to the number of (-1) or (1) segments located under the same tunneling exciton arc. In order to remove the divergence we will now proceed to a partial resummation of the perturbation series (5) by

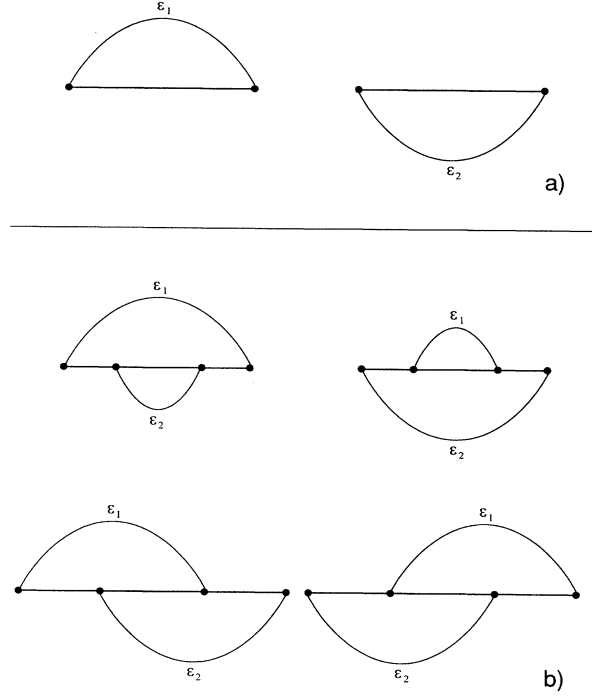


FIG. 5. (a) Lowest-order diagrams in the perturbation expansion (5) with one tunneling exciton arc. (b) Two tunneling excitons diagrams which give the perturbation expression of the cotunneling rate across the single-electron transistor.

taking into account the most diverging diagrams at each order in H_T . They are obtained when all the diverging segments belong to the same tunneling exciton [Figs. 6(a) and 6(b)]. However, we want to include in our resummation the four diagrams depicted in Fig. 5(b) in order to recover the perturbative expression of the cotunneling rate in the limit of small transport voltages. Hence it is necessary to keep also the diagrams with two different possible tunneling excitons for the (-1) and (1) segments [Figs. 6(c) and 6(d)]. One can classify these diagrams in four different types analogous to the four diagrams of Fig. 5(b). The integral corresponding to the first type of diagrams [Fig. 6(a)] is

$$I_k = \int_0^{+\infty} \frac{\lambda t_1^2 \varepsilon_1}{z - (E_1 + \varepsilon_1)} \left[\int_0^{+\infty} \frac{\lambda t_2^2 \varepsilon_2 d\varepsilon_2}{[z - (E_1 + \varepsilon_1)][z - (-eV + \varepsilon_1 + \varepsilon_2)]} \right]^k d\varepsilon_1. \quad (6)$$

With $z = 0 + i\eta$ the resummation yields

$$\sum_{k=0}^{+\infty} I_k = \int_0^{eV} \frac{\lambda t_1^2 \varepsilon_1 d\varepsilon_1}{-(E_1 + \varepsilon_1) + i\pi\lambda t_2^2 (eV - \varepsilon_1)}. \quad (7)$$

This integral can be calculated explicitly. After taking the imaginary part, we obtain the following contribution to the decay rate:

$$f(E_1, eV) = \frac{2\pi}{\hbar} \lambda^2 t_1^2 t_2^2 \left[-eV + \frac{2E_1 + eV}{2} \times \ln \frac{(eV + E_1)^2}{E_1^2 + (\pi\lambda t_2^2 eV)^2} \right] - \frac{2}{\hbar} \lambda t_1^2 E_1 \left[\pi/2 - \arctan \frac{E_1}{\pi\lambda t_2^2 eV} \right] + O(\lambda^2 t_1^2 t_2^2). \quad (8)$$

The contribution $f(E_2, eV)$ of the second type of diagrams [Fig. 6(b)] has the same form with E_1 replaced by E_2 , t_1 by t_2 , and t_2 by t_1 . In the third and fourth types of diagrams there are two possible tunneling excitons for the (-1) and (1) segments. The integrals and the resummation

are performed similarly to the previous case. Since the third and the fourth types of diagrams [Figs. 6(c) and 6(d)] are symmetric, they give the same contribution to the decay rate:

$$g(E_1, E_2, eV) = \frac{2\pi}{\hbar} \lambda^2 t_1^2 t_2^2 \left[eV - \frac{(E_1 + eV)E_1}{2(E_1 + E_2 + eV)} \ln \frac{(E_1 + eV)^2}{E_1^2 + (\pi\lambda t_2^2 eV)^2} - \frac{(E_2 + eV)E_2}{2(E_1 + E_2 + eV)} \ln \frac{(E_2 + eV)^2}{E_2^2 + (\pi\lambda t_1^2 eV)^2} \right] + O(\lambda^2 t_1^2 t_2^2). \quad (9)$$

Summing the contributions of the four types of diagrams and using Eq. (1), the final expression of the decay rate $\Gamma = f(E_1, eV) + f(E_2, eV) + 2g(E_1, E_2, eV)$ takes the form

$$\Gamma = \frac{2\pi}{\hbar} \frac{R_K^2}{(4\pi^2)^2 R_{t_1} R_{t_2}} \left[\frac{eV}{2} + \frac{E_1 E_2}{E_1 + E_2 + eV} \right] \times \left[\sum_{i=1}^2 \ln \frac{(eV + E_i)^2}{E_i^2 + (\alpha_i eV)^2} \right] - \frac{2\pi}{\hbar} \sum_{i=1}^2 \frac{R_K E_i}{4\pi^2 R_{t_i}} \left[\frac{1}{2} - \frac{1}{\pi} \arctan^{-1} \frac{E_i}{\alpha_i eV} \right], \quad (10)$$

where $\alpha_i = R_K / 4\pi R_{t_j}$, $j \neq i$. This formula provides an expression of the I - V characteristic of the single-electron transistor at $T=0$. In the limit $\alpha_i \rightarrow 0$, Eq. (10) reproduces the perturbative expression of the cotunneling rate across two junctions in series calculated by Averin and Odintsov.⁶ One can also treat second-order tunneling in any linear array of tunnel junctions if one replaces eV in Eq. (10) by the correct expression for the energy available in the transition. Expression (10) has a form similar to the cotunneling rate expression of Korotkov *et al.*¹¹ The two formulas, although analytically different, give the same result, except in the vicinity of the threshold voltage V_{th} . Recently, Pasquier *et al.*¹³ have explained their experimental results on a two-dimensional electron gas electrometer by a temperature-dependent cotunneling rate which agrees with Eq. (10) in the limit $T=0$.

IV. THE GENERAL CASE OF A CROSSOVER BETWEEN N TUNNELING AND $(N-1)$ TUNNELING IN A GENERAL LINEAR ARRAY

More generally, the crossover between N and $(N-1)$ tunneling in larger arrays than the two junctions electrometer can be described by a similar nondivergent rate calculation. We now consider a linear array of N tunnel junctions with negligible gate capacitances biased with a voltage source V (Fig. 7). In the case of N identical junctions with capacitance C the set of intermediate energies (E_1, \dots, E_{N-1}) is the same for all the sequences. For $V < e/2C$, the N tunneling is the only allowed transition. At $V = e/2C$, E_{N-1} is equal to zero and an $N-1$ tunneling transition becomes possible. An N tunneling transi-

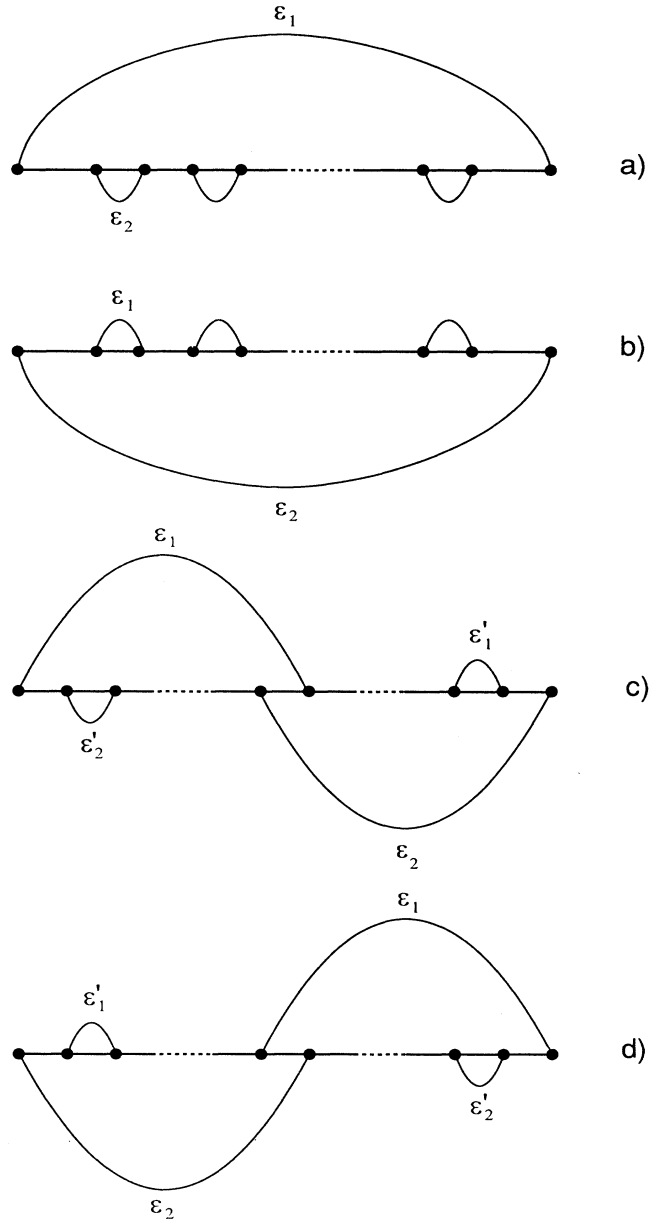


FIG. 6. Diagrams that are taken into account in the partial resummation of the perturbation expansion (5).

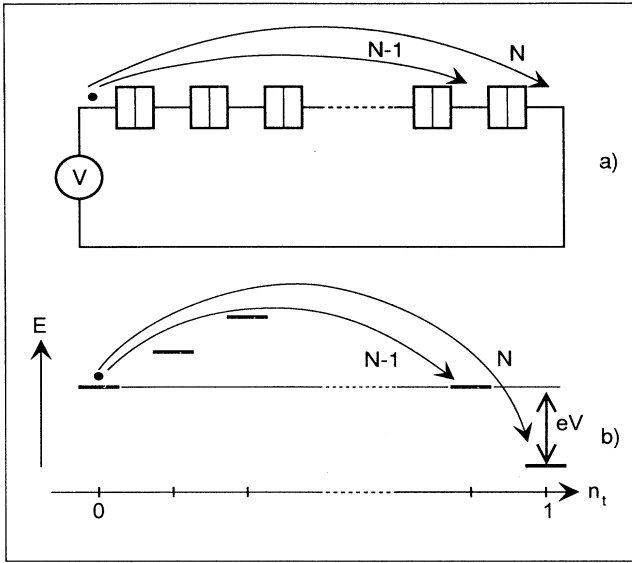


FIG. 7. Cotunneling transition (a) in real space and (b) in state space for a linear array of N identical tunnel junctions with negligible gate capacitances biased by a voltage source V when the energy of the $(N-1)$ th intermediate state of an N tunneling transition is equal to the initial-state energy.

tion is described at the lowest order in perturbation by $N!^2$ different diagrams containing N tunneling excitons. If $V \ll e/C$, the energies of the $N-2$ first intermediate states are always positive and larger than eV . Since the sum of the energies of the tunneling excitons involved in a cotunneling transition is equal to eV , we will neglect them in the energy denominators related to the configuration states of the array except for the $(N-1)$ th state and the final one. We can then distinguish only two types of diagrams (Fig. 8). There are $N!(N-1)!$ diagrams of the first type and $N!(N-1)!(N-1)$ diagrams of the second type. For the first type [Fig. 8(a)] the resummation and integral over ε_N and ε_{N-1} is performed in the same manner as in the first two cases of the single-electron transistor. Then one gets the contribution γ_a :

$$\gamma_a = \int \cdots \int_0^{+\infty} \left[\prod_{i=1}^{N-2} \frac{\lambda t^2}{E_i^2} \right] [f(E_{N-1} + \sigma, eV - \sigma)] \times \varepsilon_1 \cdots \varepsilon_{N-2} d\varepsilon_1 \cdots d\varepsilon_{N-2}, \quad (11)$$

where $\sigma = \sum_{i=1}^{N-2} \varepsilon_i$ and where f is the function defined in expression (8). For the second type of diagram [Fig. 8(b)], which is similar to the third and fourth types of diagrams in the single-electron transistor case, the contribution γ_b is

$$\gamma_b = \int \cdots \int_0^{+\infty} \left[\prod_{i=1}^{N-2} \frac{\lambda t^2}{E_i^2} \right] \times [g(E_{N-1} + \sigma, E_{N-1} + \sigma, eV - \sigma)] \times \varepsilon_1 \cdots \varepsilon_{N-2} d\varepsilon_1 \cdots d\varepsilon_{N-2}, \quad (12)$$

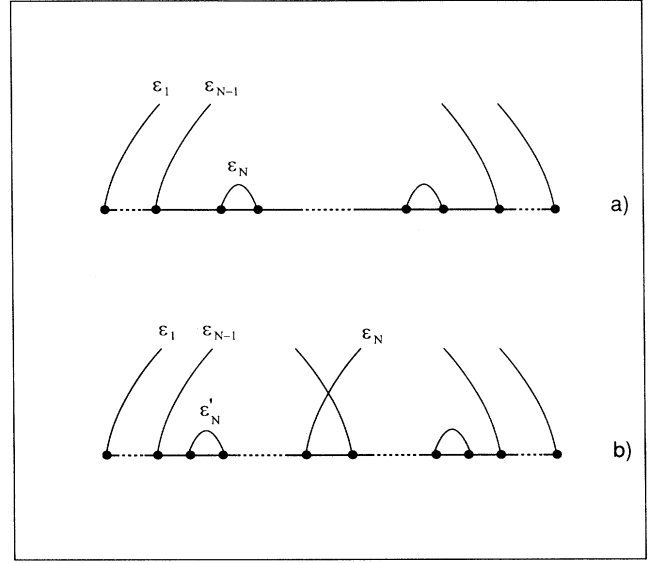


FIG. 8. Classes of diagrams for a linear array of N junctions which extend the classification made for the single-electron transistor. (a) Diagrams analogous to diagrams of Figs. 6(a) and 6(b). (b) Diagrams analogous to diagrams of Figs. 6(c) and 6(d). The arcs starting from the horizontal line represent the emission of tunneling excitons labeled $\varepsilon_1, \dots, \varepsilon_{N-1}$. The arcs ending on the horizontal line represent the absorption of the previous tunneling excitons $\varepsilon_1, \dots, \varepsilon_{N-1}$ in an arbitrary order.

where g is the function defined in expression (9). The decay rate of the initial state $\Gamma_N = \gamma_a + \gamma_b$ is written

$$\Gamma_N = \left[\frac{R_K}{4\pi^2 R_t} \right]^{N-2} N!(N-1)! \prod_{i=1}^{N-2} E_i^{-2} F(E_{N-1}, eV), \quad (13)$$

where

$$F(E_{N-1}, eV) = \int_0^{eV} \frac{\sigma^{2N-5}}{(2N-5)!} \times [f(E_{N-1} + \sigma, eV - \sigma) + (N-1)g(E_{N-1} + \sigma, E_{N-1} + \sigma, eV - \sigma)] d\sigma.$$

Equation (13) allows us to describe any kind of crossover between two tunneling regimes in a linear array of N tunnel junctions under the effect of a finite transport voltage. Thus one can estimate the I - V curve of the array from the N tunneling regime until the single tunneling regime. In the simplest case $N=3$, a quantitatively more accurate calculation can be done if one keeps in the energy denominators of expressions (11) and (12) the contribution of the first tunneling exciton energy ε_1 . One obtains the following expression of the 3 tunneling rate:

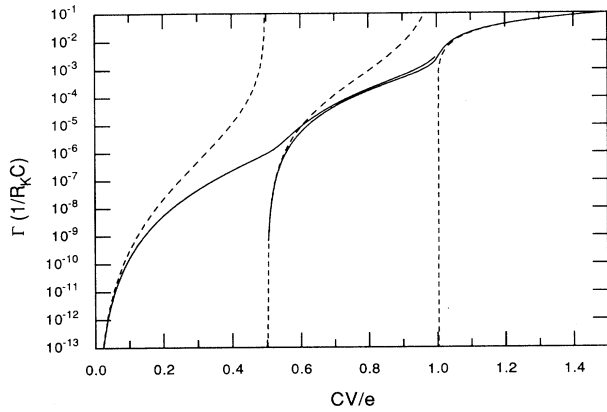


FIG. 9. Tunneling rates across a linear array of three junctions as a function of the transport voltage V . Solid lines are Γ_3 [Eq. (14)] plotted in the interval $0 < CV/e < 1$ and $3\Gamma_2$ calculated using Eq. (10) with the correct expression of the energy difference available instead of eV . Dashed lines are the divergent tunneling rates across three, two, and one junction obtained by Eq. (3) when one retains only electrostatic energies in the energy denominators. All the curves are calculated for $R_t = 10R_K$.

$$\Gamma_3 = \left[\frac{R_K}{4\pi^2 R_t} \right] 12K(E_2, eV)$$

$$\text{where } K(E_2, eV) = \int_0^{eV} \frac{f(E_2 + \varepsilon_1, eV - \varepsilon_1) + 2g(E_2 + \varepsilon_1, E_2 + \varepsilon_1, eV - \varepsilon_1)}{(E_1 + \varepsilon_1)^2} \varepsilon_1 d\varepsilon_1. \quad (14)$$

This formula Γ_3 correctly describes the 3 tunneling regime and the 2 tunneling regime until the vicinity of the single tunneling threshold. Another expression is necessary to describe the crossover between 2 tunneling and single tunneling. The 2 tunneling rate Γ_2 is evaluated using Eq. (10) with the correct expression of the available

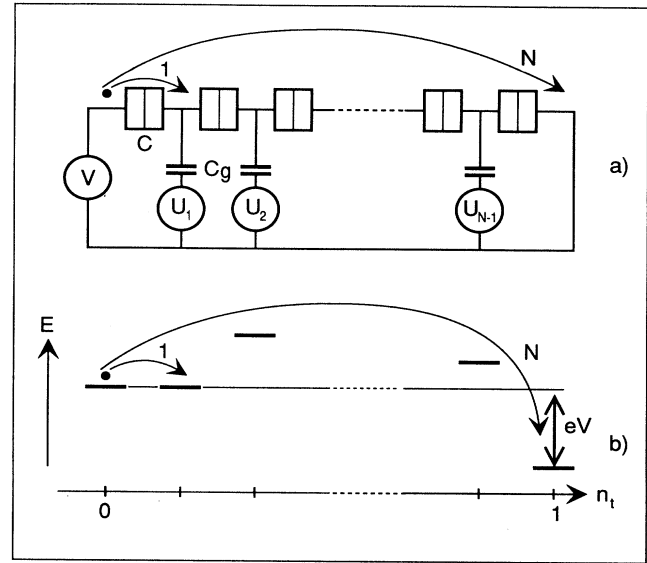


FIG. 11. Evolution of the gate voltages in the N pump during a transfer cycle of one electron charge. The amplitude of the voltage pulse is adjusted to transfer only one electron across each junction of the array.

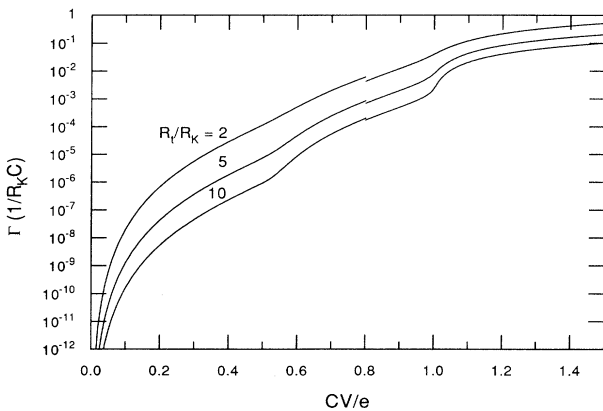


FIG. 10. Tunneling rates across a linear array of three junctions as a function of the transport voltage with $R_t = 2, 5,$ and $10 \times R_K$ from the upper to the lower curve. The curves are Γ_3 for $CV/e < 0.8$ and $3\Gamma_2$ for $CV/e > 0.8$, where Γ_3 and Γ_2 are calculated in the same way as in Fig. 9.

energy difference in place of eV . Because there are three different ways to associate two junctions of the circuit, the tunneling rate across the whole array of three junctions near the single tunneling threshold $CV/e = 1$ is given by $3\Gamma_2$. Results are shown in Fig. 9 for a particular value of the tunnel resistance $R_{t_1} = R_{t_2} = 10R_K$. For

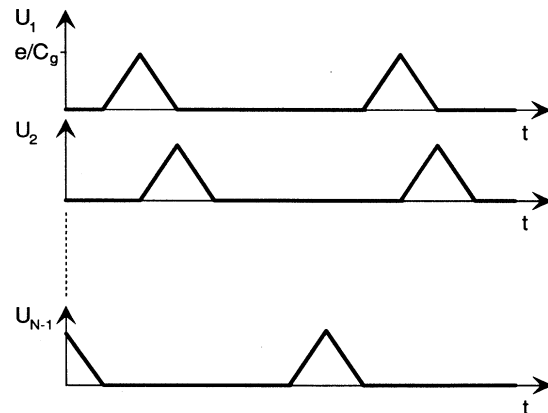


FIG. 12. (a) Circuit diagram of the N junctions pump. (b) Energy states of the array at the crossover between single tunneling across the first junction and N tunneling across the whole array.

$1/2 < CV/e < 1$ the matching between Γ_3 and $3\Gamma_2$ is sufficiently good to obtain a continuous estimate of the tunneling rate across three junctions over the Coulomb blockade range. Calculation of the tunneling rate across three junctions is shown in Fig. 10 for several values of the tunnel resistance. The crossover between successive tunneling regimes gets smoother when the tunnel resistance R_t decreases and is hardly noticeable when $R_t < 2R_K$.

V. THE CROSSOVER BETWEEN N TUNNELING AND SINGLE TUNNELING

The last application of the nondivergent cotunneling rate calculations we shall consider deals with the accuracy of single-electron pumps.⁴ A pump consists of a linear array of N identical tunnel junctions of capacitance C where each island $\{k\}$ of the array is connected through a gate capacitor to a time-dependent voltage source U_k (Fig. 11). Each gate capacitance is equal to C_g with $C_g \ll C$. The controlled transfer of one electron across the device is achieved by successively applying to the islands triangular voltage pulses as shown in Fig. 12. These pulses induce a sequence of single tunneling events on the successive junctions of the array: one-electron charge follows the pulse propagation through the array. However, an unwanted N tunneling transition is possible at any stage of the transfer cycle. All steps of a transfer cycle in the N pump are equivalent,¹⁶ but, for simplicity, let us assume the pump is placed at the beginning of a cycle. There is no excess electron on any island of the array and at small transport voltages ($V \ll e/2C$) the N tunneling across the array is the only tunneling transition allowed. As in the single-electron transistor, the perturbative expression of this N tunneling rate diverges when the energy of the first intermediate state of a cotunneling sequence becomes equal to zero. This is exactly what happens when, under the effect of the first gate voltage U_1 , the pump reaches the threshold of the first step in the cycle. This step will be a single tunneling event across the first junction which puts one excess electron on the first island of the array in the sense of the transfer (Fig. 11). The perturbation theory cannot therefore be used directly to calculate the pump error rate. Using the partial resummation technique we can remove the divergence of the N tunneling rate. The general form of the diverging diagrams is represented in Fig. 13. Introducing the same approximation as in the case of the N linear array of tunnel junctions we neglect the tunneling exciton energies in the energy denominators except for the first intermediate state. After the resummation and the integration over the tunneling exciton energies $\varepsilon_2, \dots, \varepsilon_N$, we obtain the

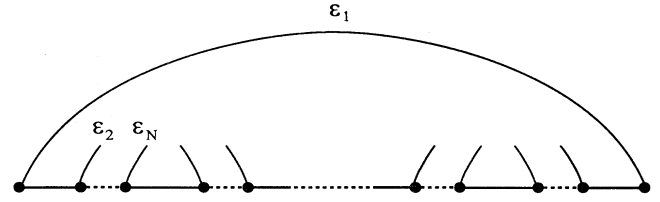


FIG. 13. Diverging diagrams involved in the resummation of the perturbation series in the case of the crossover between N tunneling and single tunneling in the N junctions pump.

following upper bound of the N tunneling rate γ_{err} :

$$\gamma_{\text{err}} = \frac{N!^2}{(2N-3)!} \frac{2\pi}{\hbar} \left[\frac{R_K}{4\pi^2 R_t} \right]^N \left[\prod_{i=2}^{N-1} E_i^{-2} \right] \times \int_0^{eV} \frac{\varepsilon_1 (eV - \varepsilon_1)^{2N-3} d\varepsilon_1}{(E_1 + \varepsilon_1)^2 + \alpha_N^2 (eV - \varepsilon_1)^{4N-6}},$$

where $\alpha_N = \frac{\pi}{(2N-3)!} \left[\frac{R_K}{4\pi^2 R_t} \right]^{N-1} \prod_{i=2}^{N-1} E_i^{-2}$. (15)

Using this expression, we have calculated in the particular case of the five junctions pump an upper bound of the N tunneling leakage during a transfer cycle. We have found that this contribution is negligible in the particular parameter range for which metrological accuracy is achievable.^{17,18,16}

VI. CONCLUSION

In conclusion we have shown that in a linear array of tunnel junctions the problem of the crossover between two tunneling regimes at different orders can be solved by a partial resummation of the perturbation expansion. In the case of the single-electron transistor, we have obtained an analytical expression of the cotunneling rate that remains finite at the conduction threshold. More generally, this approach can be used to calculate the I - V characteristic of an array. Finally, nondivergent calculation of the cotunneling rate provides a rigorous upper bound on the N tunneling leakage through charge-transferring devices such as the N junctions pump.

ACKNOWLEDGMENTS

We acknowledge fruitful discussions with M. H. Devoret, H. Grabert, P. Joyez, J. M. Martinis, and H. Pothier.

¹D. V. Averin and K. K. Likharev, in *Mesoscopic Phenomena in Solids*, edited by B. Al'tshuler, P. Lee, and R. Webb (Elsevier, Amsterdam, 1991), Chap. 6; *Single Charge Tunneling*, edited by H. Grabert and M. H. Devoret (Plenum, New York, 1992).

²T. A. Fulton and G. J. Dolan, Phys. Rev. Lett. **59**, 109 (1987).

³L. J. Geerligs, V. F. Anderegg, P. A. M. Holweg, J. E. Mooij,

H. Pothier, D. Esteve, C. Urbina, and M. H. Devoret, Phys. Rev. Lett. **64**, 2691 (1990).

⁴H. Pothier, P. Lafarge, D. Esteve, C. Urbina, and M. H. Devoret, Europhys. Lett. **17**, 249 (1992).

⁵K. A. Matveev, Zh. Eksp. Teor. Fiz. **99**, 1598 (1991) [Sov. Phys. JETP **72**, 892 (1991)].

- ⁶D. V. Averin and A. A. Odintsov, *Phys. Lett. A* **149**, 251 (1989).
- ⁷L. J. Geerligs, D. V. Averin, and J. E. Mooij, *Phys. Rev. Lett.* **65**, 3037 (1990).
- ⁸T. M. Eiles, G. Zimmerli, H. D. Jensen, and J. M. Martinis, *Phys. Rev. Lett.* **69**, 148 (1992).
- ⁹M. H. Devoret, D. Esteve, H. Grabert, G.-L. Ingold, H. Pothier, and C. Urbina, *Phys. Rev. Lett.* **64**, 1824 (1990).
- ¹⁰M. Ueda and F. Guinea, *Z. Phys. B* **85**, 413 (1991).
- ¹¹A. N. Korotkov, D. V. Averin, K. K. Likharev, and S. A. Vasenko, in *Single-Electron Tunneling and Mesoscopic Devices*, edited by H. Koch and H. Lübbig (Springer, Berlin, 1992).
- ¹²Yu. V. Nazarov, *J. Low-Temp. Phys.* **90**, 77 (1993); W. Krech and A. Hädicke, *Int. J. Mod. Phys. B* **7**, 2201 (1993).
- ¹³C. Pasquier, U. Meirav, F. I. B. Williams, D. C. Glatli, Y. Jin, and B. Etienne, *Phys. Rev. Lett.* **70**, 69 (1993).
- ¹⁴L. O. Kulik and R. I. Shekter, *Zh. Eksp. Teor. Fiz.* **68**, 623 (1975) [*Sov. Phys. JETP* **41**, 308 (1975)].
- ¹⁵C. Cohen-Tannoudji, J. Dupont-Roc, and G. Grynberg, *Atom-Photon Interactions. Basic Processes and Applications* (Wiley, New York, 1992), Chap. 3.
- ¹⁶H. Pothier, P. Lafarge, D. Esteve, C. Urbina, and M. H. Devoret, *IEEE Trans. Instrum. Meas.* **42**, 324 (1993).
- ¹⁷H. D. Jensen and J. M. Martinis, *Phys. Rev. B* **46**, 13407 (1992).
- ¹⁸D. V. Averin, A. A. Odintsov, and S. V. Vyshenskii, *J. Appl. Phys.* **73**, 1297 (1993).